Bond behavior of NSM CFRP laminates in concrete under sustained loading

M. Emara[a,b,*], C. Barris[a], M. Baena[a], L. Torres[a], and J. Barros[c]

[a]*AMADE, Polytechnic School, Universitat de Girona, Campus Montilivi s/n, 17003 Girona, Spain*
[b]*Structural Engineering Dept., Faculty of Engineering, Zagazig University, B.O. Box 44519, Zagazig, Sharkia, Egypt.*
[c]*ISISE, University of Minho, Department of Civil Engineering, Campus de Azurém, 4800-058 Guimarães, Portugal*

Abstract

The success of Fiber Reinforced Polymers (FRP) strengthening methodologies for reinforcing concrete structures is highly related to the interfacial bond properties between reinforcement and concrete, which depends upon a number of parameters. Several studies were carried out investigating the short-term bond behavior of Near Surface Mounted (NSM) FRP strengthening systems. However, there has been only limited investigation of its long-term behavior resulting in a significant lack of available experimental data about this relevant aspect. The bond performance of the materials involved in the NSM FRP strengthening system (FRP, adhesive and concrete), due to its nature, is susceptible to be affected by both the sustained loading and environmental conditions. In this study, bond of NSM Carbon FRP (CFRP) laminates in concrete was investigated experimentally using pull-out tests. The experimental program consisted of both short-term tests, in which the load was applied monotonically up to failure, and long-term tests in which different levels of sustained loading were applied. The specimens were tested under sustained loading using bonded length,

---

*Corresponding author. Tel: +34 627114755
Email addresses: mohamed.emara@udg.edu (M. Emara), cristina.barris@udg.edu (C. Barris), marta.baena@udg.edu (M. Baena), Lluis.torres@udg.edu (L. Torres), barros@civil.uminho.pt (and J. Barros)

adhesive thickness and sustained loading level as the main parameters of the study. Results in terms of slip evolution with time are presented to explore the effects of the studied parameters on the long-term bond behavior between NSM CFRP laminates and concrete. Moreover, an analytical procedure to predict the slip variation versus time is proposed and compared to experimental results.

1. Introduction

The use of Fiber Reinforced Polymer (FRP) reinforcement in the strengthening of Reinforced Concrete (RC) structures has received considerable attention within the civil and structural engineering fields. Their unique properties, such as the high strength-to-weight ratio and excellent corrosion resistance, make them a suitable and effective alternative to conventional steel for both reinforcing and strengthening purposes [1–5].

The most common techniques for strengthening RC structures using FRP materials are those usually known as Externally Bonded Reinforcement (EBR) and Near Surface Mounted (NSM) reinforcement [3, 6–14]. Recently, researchers have shown an increased interest in the NSM technique due to several potential advantages, such as: (i) less prone to debonding from the concrete substrate, (ii) does not require any surface preparation work except grooving, (iii) being the FRP reinforcements better protected by the concrete cover, this technique is then suitable to strengthen the negative moment regions of beams and slabs, and (iv) the aesthetics of a strengthened structure with NSM reinforcement are virtually unchanged [8, 15].

Surveys such as those reported in [8, 16, 17] showed that Carbon FRP (CFRP) has been used in most existing studies for NSM strengthening of concrete structures. CFRP reinforcement has higher tensile strength and elastic modulus compared to other

available FRP materials, resulting in some advantages such as: use of smaller cross-sectional area, need of smaller groove size, and reduction in the amount of the groove filling material.

Bond between FRP and concrete is a fundamental property that influences the success and the efficiency of the strengthening system as it controls the composite action development between both materials [18–20]. Besides, it affects the load carrying capacity, spacing and width of cracks, as well as the failure mode of the strengthened member [21].

Many parameters may affect the bond behavior and load capacity of the NSM procedure, bonded length, groove size and adhesive properties being among those more influencing [17, 22–28].

Bond tests (direct pull-out and beam-pull out tests) adapted from those existing for steel RC can be used to determine the bond capacity of the strengthening system and concrete splitting resistance along the reinforcement. The direct pull-out test is one of the most common types of bond tests due to its simplicity and advantages: (i) specimens can be easily manipulated, (ii) the area of interest can be easily inspected and (iii) variety of tests specimens and setups can be used [29, 30]. Direct pull-out tests can be divided into two main types: single-shear pull-out test, in which one concrete block is used and the FRP reinforcement is bonded to one face of the specimen having the advantage of simple preparation; and double-shear pull-out test, in which one or two concrete blocks are used and the FRP reinforcements are bonded to two opposite faces of the specimen. Although double-shear pull-out test is considered a way to overcome the eccentricity of the reinforcement, single-shear configuration has been more widely used due to its simplicity in preparation and inspection (some issues related to preparation and execution may affect the possible advantages of double-shear configuration: eccentricities, influence of embedded steel bars, or the need to measure

3

in both reinforcements). A more detailed analysis of these tests is provided elsewhere [17, 31–34]. Another issue related to the performance of direct pull-out tests is the presence of compression in the concrete in the most classical setup of the test, which may introduce some confinement affecting the bond performance (also for steel RC). However the possible effect of this confinement may depend on the interrelation between geometrical and mechanical parameters of the test and was not always found to be present [17]. It can be said that most of the studies carried out used the single-shear pullout test due to its simplicity. Although its specific setup may not exactly represent the conditions in strengthened elements, it has been considered an effective method to obtain results able to quantify, check and compare the bond performance of different joint configurations.

A primary concern of strengthened RC structures performance is its long-term bond behavior under serviceability limit state (SLS) conditions, which may be affected by several parameters in case of NSM systems. The impact of adhesive properties on the long-term bond behavior between NSM CFRP strips and concrete was investigated and reported in [35], where the temperature, the adhesive curing time and the initial tensile strip force were the test variables. Results showed that the creep effects were reduced due to the increase in the adhesive curing period, and that the creep was dependent on the stress level in the adhesive layer. In addition, the system performance was affected significantly due to the exposure to high temperature. In the same study, a model to simulate the interaction between adhesive and bond of NSM FRP strips was introduced. The model was based on the non-linear bond-slip law (composed of four different regions) presented in [36] and used for bond of deformed steel bars in concrete.

Costa and Barros [37] have investigated experimentally and analytically the creep effects on NSM systems applied with a certain prestress level and concluded that up to sustained stress levels of 60% the adhesive endured up two times the instantaneous

4

strain without rupturing. Since the reduction of the values of the Kelvin components was verified, the time period between adhesive production and its application is a relevant aspect for maintaining the aimed prestress level in the NSM CFRP systems.

With the aim of studying the durability of RC elements strengthened with the NSM technique, Silva et al. [38] experimentally tested beam pull-out and slab specimens strengthened with NSM CFRP strips under sustained loading. Some specimens were kept in the laboratory conditions, others were immersed in water containing 0% and 3.5% of chlorides, while others were subjected to wet/dry cycles. The effect of creep was found to be practically negligible in the case of beam pull-out specimens; however, a noticeable creep effect was observed in case of slab specimens.

Derias et al. [39] studied the durability of RC beams strengthened with NSM CFRP strips. Sustained load equal to 40% of the ultimate load carrying capacity was applied. Some beams were subjected to high temperature, while some others were left in room conditions. Results showed deterioration in the epoxy-concrete interface and changes in failure modes due to the extreme environmental conditions.

On the other hand, numerous works have been carried out to study the long-term bond behavior between CFRP plates Externally Bonded (EB) to concrete blocks. Mazzotti and Savoia [40] tested double shear pull-out specimens under sustained loading equal to 50% of the ultimate load using three different bonded lengths. Significant redistribution of the shear stresses was observed along the bonded length due to the creep deformation. Based on the experimental results, a simplified model was proposed to predict the evolution of strain and shear stress with time for EBR. The model was developed by using the effective modulus (EM) method, and a linear bond-slip law to model the FRP-concrete anchorage.

Meshgin et al. [41] performed an experimental study in which the effect of applied sustained stress, epoxy thickness and epoxy curing time before loading, on the long-

term behavior of EB FRP plates was analyzed. Results revealed that the applied sustained stress (as a percentage of the ultimate stress) and the epoxy curing time before loading could be the most critical parameters affecting creep of epoxy at the concrete-FRP interfaces. Similar conclusions were observed in NSM CFRP systems by Costa and Barros [37]. Furthermore, it was observed that more creep was developed as the applied sustained stress increased, so that the application of high sustained stress levels may result in unexpected failures. Based on the experimental results, a modification of the Maxwell creep model was suggested in order to model the long-term behavior of epoxy at the interfaces. By modifying the Burger's model, taking into account the experimental creep test results, Costa and Barros [37] demonstrated the good applicability of this approach for predicting the long-term behavior of NSM CFRP systems.

Dash et al. [42] performed an experimental program concerning the time-dependent deformation of EB CFRP sheets bonded to concrete surface. Single shear pull-out specimens were subjected to sustained loading equal to 40% of the ultimate load. Some of the specimens were subjected to different environmental conditions of temperature and relative humidity, while some others were immersed in water. Larger creep displacements were observed in case of specimens exposed to elevated temperature with the presence of sustained loading, as well as in those immersed in water compared to those exposed to high humidity.

Results of the study reported in [43] show that, in case of EBR, increasing the thickness of the adhesive layer helped in reducing the peak shear stress over time due to creep. They also observed that transfer length increased with time due to the presence of sustained load.

The long-term bond behavior of strengthened RC structures under SLS conditions is a key aspect that influences the performance of an FRP strengthened RC structure.

The review of the existing literature provides evidence that up to date there has been limited investigation concerning the long-term bond behavior of NSM FRP strengthening, with the consequent lack of available data and of studies about the effect of the influencing parameters. This paper presents the results of an experimental program aimed to investigate the time-dependent bond behavior between NSM FRP and concrete considering sustained load level, bonded length and adhesive thickness as the main parameters of the study. Results in terms of slip evolution with time are presented and discussed. Moreover, an analytical procedure to predict the slip variation versus time is proposed. The experimental results are satisfactorily compared to those obtained with the proposed model.

2. Experimental program

In this experimental program, single shear pull-out specimens were used to obtain the bond-slip response of NSM FRP strengthened elements due to its simplicity, as mentioned previously. Some specimens were tested under monotonic loading up to failure and others under sustained loading. The parameters of the study were the sustained loading level (25% and 50% of the failure load), the groove width (5 and 10 mm) and the bonded length (60, 90 and 120 mm). The bonded lengths were selected based on the available literature to introduce bonded lengths shorter, equal and longer than the expected effective bonded length. The effective bonded length of the system was calculated as 90 mm, based on the equations presented in [44], and similar value was reported in [45]. The slip evolution with time under the different loading and environmental conditions were monitored during the test period (i.e. 1000 hours).

For both monotonic pull-out and long-term pull-out test setups, a steel plate having a groove of 30 mm × 30 mm allowing the CFRP laminate to pass through, was placed at the top of the concrete specimen to restrain its movement when applying the pull-

7

out force. An unbonded length of 50 mm was left from the top of the concrete block to improve the behavior in front of possible premature splitting, confinement stresses and simulation of intermediate crack debonding [18, 31, 46–48].

2.1. Material properties

Specimens were cast with ready mixed concrete with compressive strength of 32 MPa (CoV 1.5%) obtained by testing three concrete cylinders of 150 mm diameter and 300 mm height (28 days after casting) in accordance with UNE 12390-3 [49]. The concrete tensile strength and modulus of elasticity were 3 MPa (CoV 1.6%) and 31 GPa (CoV 2%), respectively. The commercially produced CFRP strips from Clever Reinforcement Iberica with 1.4 mm thickness and 10 mm width were used as FRP reinforcing material. The CFRP strips were tested in accordance with ISO 527-5 [50], and a tensile strength of 2400 MPa (CoV 3.8%) and a modulus of elasticity of 160 GPa (CoV 2%) were obtained. According to manufacturer's recommendations, the two components epoxy resin under the commercial name of S&P220 was used for bonding the laminates to concrete. The tensile strength and modulus of elasticity of the adhesive used were obtained (after 10 days of curing at 20 °C and 55% RH) in accordance with ISO 527-2 [51], and were found to be 20 MPa (CoV 2.3%) and 6600 MPa (CoV 2.5%), respectively.

2.2. Specimen's preparation

Eighteen concrete blocks with the dimensions equal to 200 mm × 200 mm × 250 mm, as shown in Fig. 1, were cast and cured under normal laboratory conditions. Once cured, grooves (adapted to the required width and 15 mm depth) were cut and cleaned with compressed air. Both components of epoxy were mixed, in a proportion of 4A:1B (in weight), until a uniformly gray color (without any streaks) was obtained. Once prepared, the groove was filled with resin to the required bonded length, followed by

¹⁷⁴ the placement of the laminate into the groove. Finally, the surface was leveled and the

¹⁷⁵ resin was left for curing 10 days before testing at the conditions of $20\,°C$ and 55% RH.
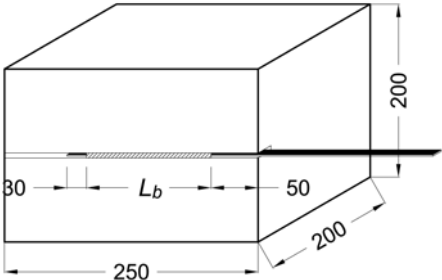

Fig. 1: Test specimen configuration (units in mm)

¹⁷⁶

2.3. Monotonic pull-out test

¹⁷⁸ Single shear specimens, with three different bonded lengths (L_b=60, 90 and 120

¹⁷⁹ mm) were tested under direct pull-out shear test (Fig. 2) to obtain their failure loads.

¹⁸⁰ For every bonded length, three specimens were tested, thus making a total of nine

¹⁸¹ single shear pull-out tests. Two LVDTs were used to measure the loaded and free end

¹⁸² slips. The load was applied using a servo-hydraulic testing machine with displacement

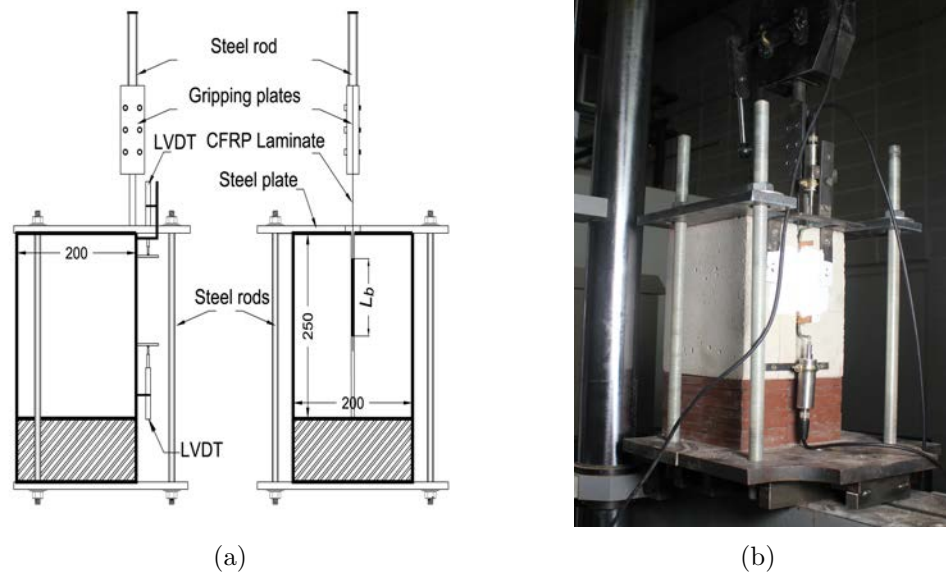¹⁸³ controlled rate of 0.2 mm/min.

9

Fig. 2: (a) Sketch of short-term setup (units in mm) and (b) test setup

2.4. Long-term pull-out test

A total of nine specimens were tested under sustained loading conditions. Similarly to the short-term tests, three different bonded lengths (60, 90 and 120 mm) were considered. The sustained load to be applied was defined as 25% and 50% of failure load found in the short-term monotonic pull-out shear tests described in the previous section. The load was applied by means of gravity loading systems through special designed frames as shown in Fig. 3. These frames had a magnification factor of 8.3 and the load was applied by using small concrete blocks. With the aim to analyze the effect of the groove width, three additional tests were performed, whose groove width was doubled. Specimens were kept loaded, for 1000 hours, in a climatic chamber at 20 °C of temperature and 55% of relative humidity. Test specimens were identified as follows: the letter L followed by the bonded length in mm, the letter S followed by the percentage of applied stress level, and finally, the letter G followed by the groove width used in mm (see Table 1). The general instrumentation in these long-term pull-out

tests consisted on two LVDTs that measured the loaded and free end slips.
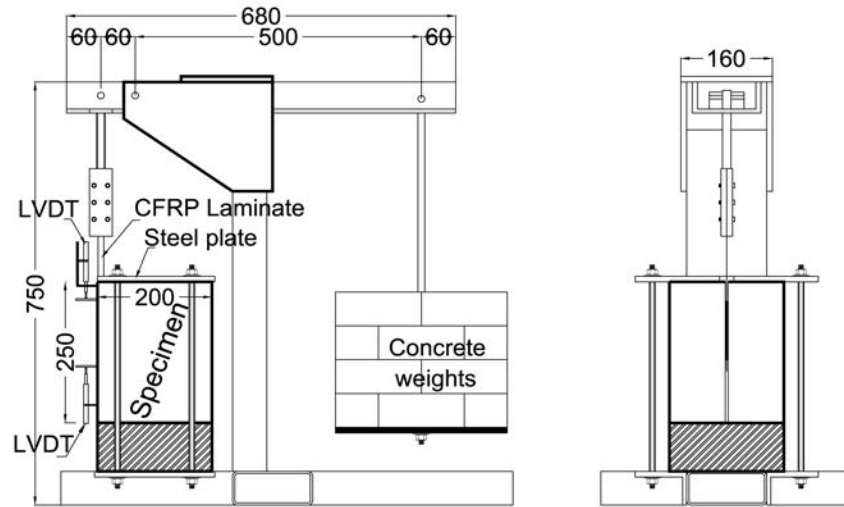
(a)

(b)

Fig. 3: (a) Sketch of sustained loading frame (units in mm) and (b) test setup

Table 1: Test matrix.

Specimen ID	Bonded length (mm)	Load level (%)	Groove width (mm)
L60S25G5	60	25	5
L90S25G5	90	25	5
L120S25G5	120	25	5
L60S50G5	60	50	5
L90S50G5	90	50	5
L120S50G5	120	50	5
L60S50G10	60	50	10
L90S50G10	90	50	10
L120S50G10	120	50	10

3. Results and discussion

3.1. Monotonic loading

Fig. 4 shows the experimental load-slip curves for the direct short-term tests. Each curve was extracted from average results of specimens tested for each bonded length (60, 90 and 120 mm).

The average load carrying capacities were 25 kN for specimens with L_b equal to 60 mm and 30 kN for specimens with L_b equal to 90 mm and 120 mm. Specimens with L_b equal to 60 mm failed by concrete failure, while specimens with L_b equal to 90 mm and 120 mm showed similar behavior but failing by FRP rupture (see Fig. 5).
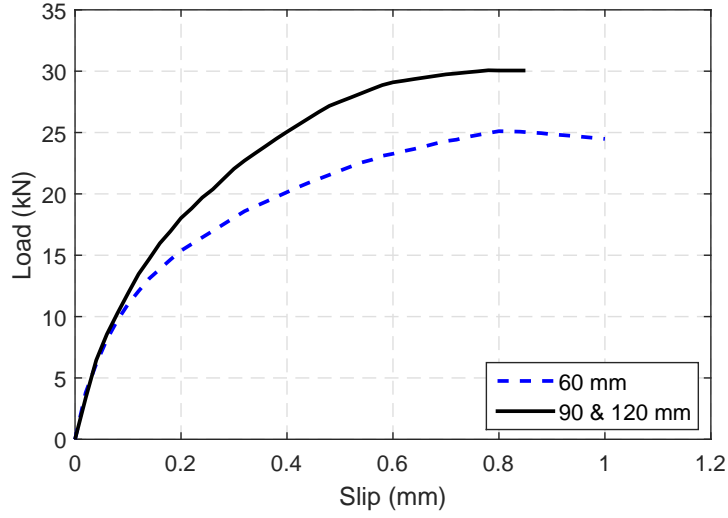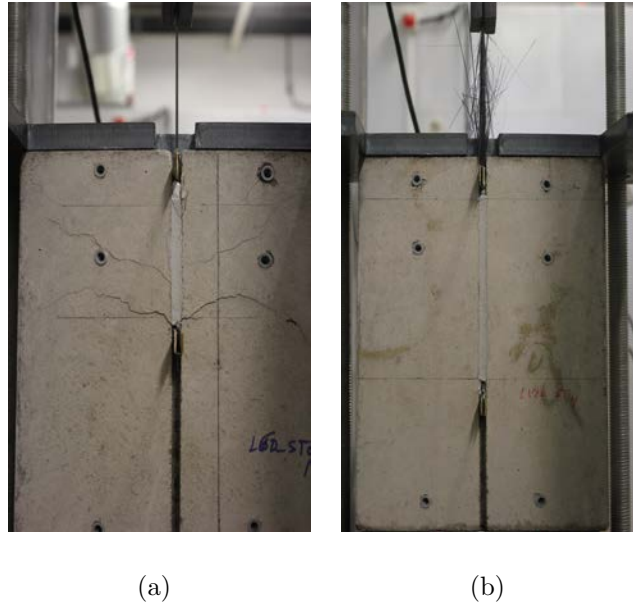
Fig. 4: Load vs. loaded end slip for short-term tests

(a)   (b)

Fig. 5: Failure modes (a) Concrete failure (L_b=60 mm) and (b) CFRP rupture (L_b=90 and 120 mm).

3.2. Sustained loading

The total slip values due to sustained loading were registered along the testing period (i.e. 1000 hours) for each specimen. Fig. 6 shows the evolution of the total

loaded-end slip with time due to the application of a sustained loading level equal to 25% of the failure load. When this sustained load was applied, similar evolution of slip was observed for specimens with bonded length equal to 90 mm and 120 mm (i.e. specimens L90S25G5 and L120S25G5, respectively). This similar behavior indicates that the bonded length was not fully activated. For shorter bonded length (i.e. specimen L60S25G5), lower total slip values were obtained as lower value of sustained loading was applied according to the percentage of the failure load.
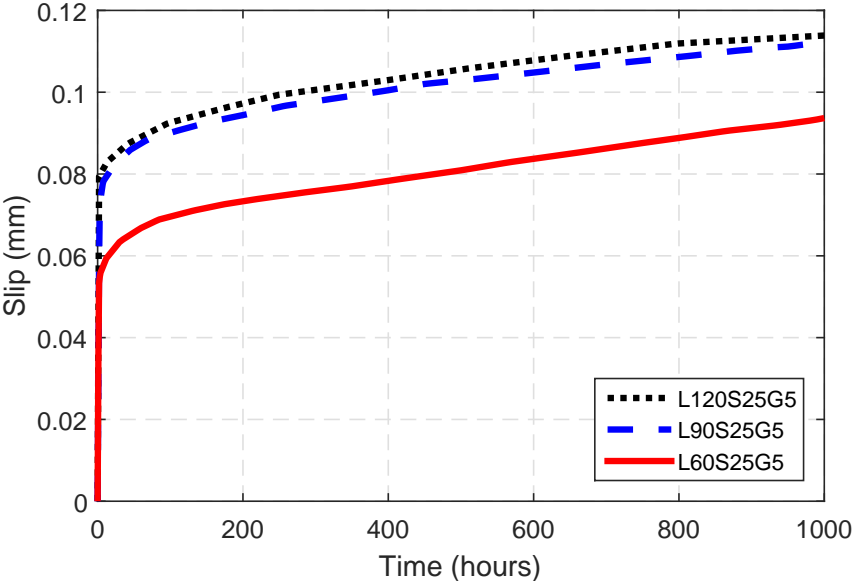

Fig. 6: Total loaded-end slip with time at sustained load level of 25%

The experimental slip evolution with time at sustained load level equal to 50%, for the case of specimens with groove width equal to 5 mm, is presented in Fig. 7. Again, similar behavior was observed for specimens having L_b equal to 90 mm and 120 mm, being the initial slip of these specimens larger than that of L_b equal to 60 mm, being this observation in agreement with that obtained from the short-term tests. Taken together (i.e. Fig. 6 and Fig. 7), the maintained similarity in the behavior of specimens with L_b equal to 90 mm and 120 mm indicate that up to sustained loading level equal to 50%

14

²²⁵ of the failure load, the bonded length was not fully activated. Similar tendencies were
²²⁶ observed in case of increasing the groove width at sustained loading equal to 50% that
²²⁷ can be shown in Fig. 8, which illustrates the total slip with time due to the application
²²⁸ of sustained loading equal to 50% of the failure load for the case of specimens with
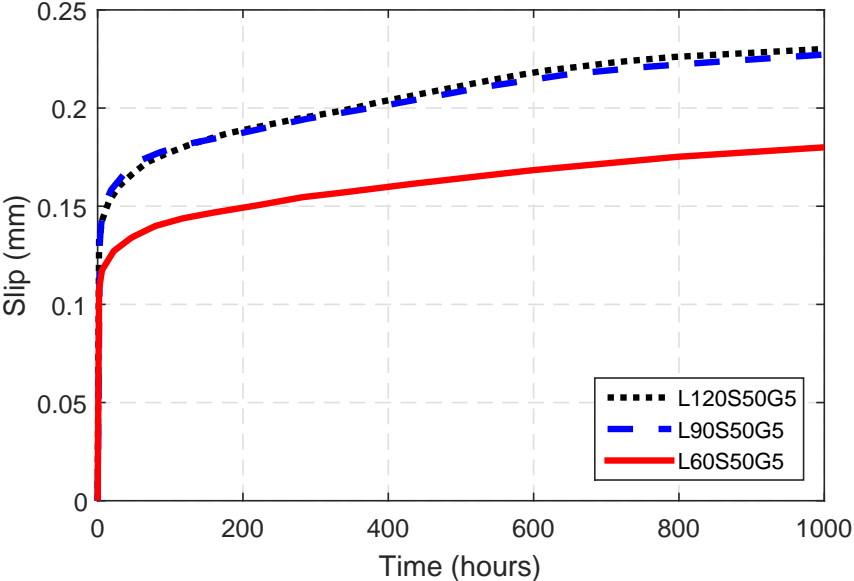groove width equal to 10 mm.

Fig. 7: Total loaded-end slip with time at sustained load level of 50 % (groove width =5 mm)

²²⁹

²³⁰   When the applied sustained loading level increased from 25% to 50%, the total slip
²³¹ increased, for all specimens by almost constant ratio of increase along the test period
²³² equal to 2.03, 2.06 and 2.07 for specimen with L_b equal to 60 mm, 90 mm and 120 mm,
²³³ respectively. It can be concluded that doubling the sustained loading level, doubled
²³⁴ the total slip at any time along the test period. This finding supports results from the
²³⁵ monotonic test (Fig. 4) in which up to 50% of the failure load, the behavior was almost
²³⁶ linear. On the other hand, increasing the groove width from 5 mm to 10 mm slightly
²³⁷ reduced the total slip values for all bonded lengths. This might be attributed to the
²³⁸ better and more homogeneous redistribution of shear stress along the bonded length
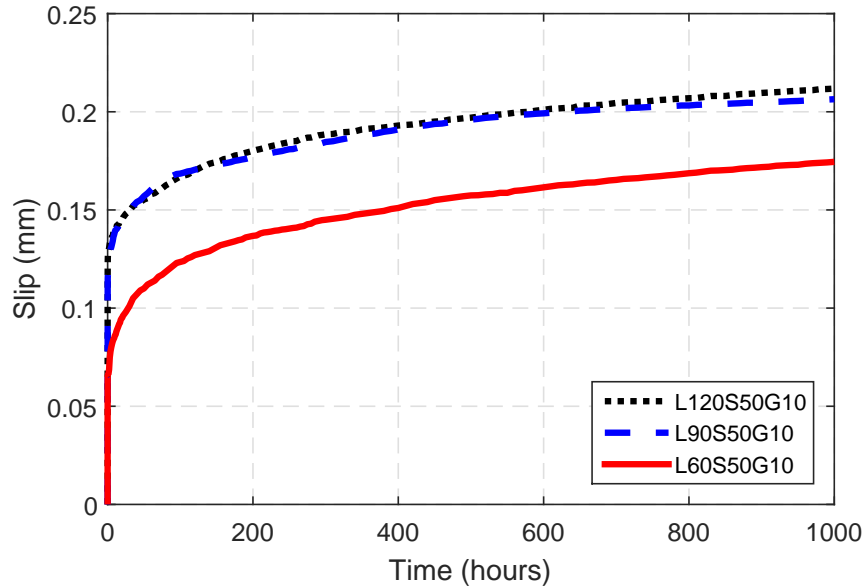
15

Fig. 8: Total loaded-end slip with time at sustained load level of 50 % (groove width =10 mm)

as a result of increasing the adhesive thickness [19, 43]. Increasing the groove width reduced the average total slip by 18%, 9% and 7% for specimen with L_b equal to 60 mm, 90 mm and 120 mm, respectively.

Experimental data presented in this study show that at a sustained load of 25% of the failure load, the ratio between the total slip at 1000 hours of sustained loading to the instantaneous slip at the time of application of the sustained load (t=0) was found to be 1.77, 1.77 and 1.88 for specimens L60S25G5, L90S25G5 and L120S25G5, respectively. When sustained loading equal to 50% was applied, similar ratios were obtained with values of 1.75, 1.76 and 1.75 in case of specimens L60S50G5, L90S50G5 and L120S50G5, respectively. On the the other hand, the ratio slightly increased, to be 2.1, 1.82 and 1.83 for specimens L60S50G10, L90S50G10 and L120S50G10, respectively, when the groove width increased from 5 to 10 mm. It was observed that the obtained ratios were almost constant for all cases, however a slight increase was found, as a result of increasing the adhesives volume, when the groove width increased. This slip

16

creep increase ratio is directly related to the tensile creep of the adhesive, since for this time period and stress level in the adhesive, Costa and Barros [37] and Emara et al. [52] have measured a tensile strain between two and three times the instantaneous one. No visible changes were appreciated in the appearance of the specimens during the test. By the end of testing period, specimens were unloaded and there were no visible cracks or signs indicating failure either in the concrete or in the epoxy.

4. Analytical modeling

In this section a simplified procedure to simulate the long-term behavior, under SLS conditions and sustained loading, of the NSM joint is proposed. First the governing equations for short-term bond behavior are described and then the simulation of the long-term behavior is introduced.

4.1. Short-term bond behavior

In a monotonic pull-out test, forces are transferred from reinforcement to concrete through the adhesive by means of shear stresses that appear at their interfaces. Fig. 9 shows an infinitesimal element of CFRP strip of length dx, showing the shear stresses at the interface and tensile stresses at the transversal section (of dimensions h_f x t_f).

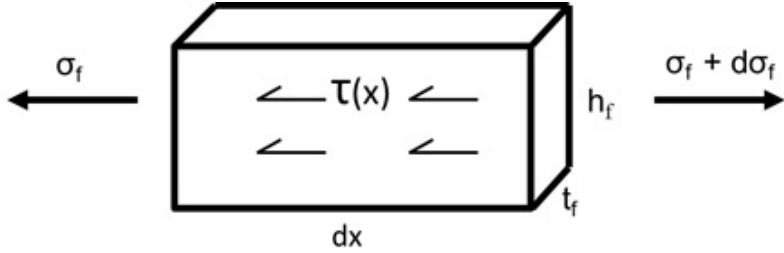Fig. 9: Infinitesimal element of NSM strip

Equilibrium equation of this infinitesimal element, along with the assumption of CFRP strip having a linear elastic behavior and CFRP-concrete joint being at the

₂₇₁ elastic stage, allows obtaining the differential equation governing the stress transfer

₂₇₂ process (Eq. 1):

$$\frac{d\sigma_f}{dx} = \frac{\tau(x)}{t_{eq}} \tag{1}$$

₂₇₃

$$t_{eq} = A_f / L_p \tag{2}$$

$$L_p = (t_f + t_a) + 2(h_f + t_a) \tag{3}$$

₂₇₄ where σ_f is the tensile stress in the FRP, τ is the shear stress, t_{eq} is the ratio between

₂₇₅ the FRP cross-sectional area (A_f) and the intermediate perimeter in the adhesive layer

₂₇₆ (L_p), t_a is the thickness of the adhesive layer, and t_f and h_f are the thickness and the

width of the FRP strip, respectively (see Fig. 10).
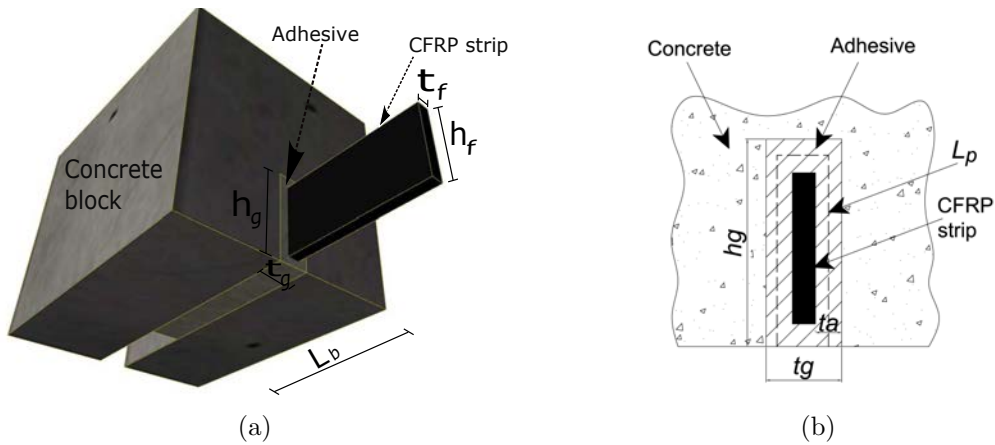

Fig. 10: (a) NSM system and (b) Details of cross section.

₂₇₇

₂₇₈ According to the literature [8, 17, 40, 44, 53–59], the bond-slip behavior of FRP

₂₇₉ reinforced elements can be satisfactorily simulated by using a local bilinear law as that
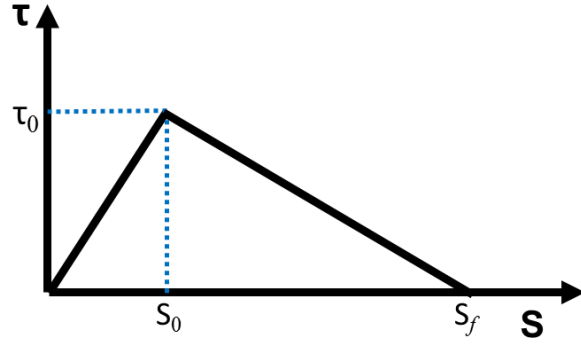
Fig. 11: Bi-linear bond-slip

shown in Fig. 11 and described by Eq. 4.

$$\tau = \begin{cases} \frac{\tau_0}{s_0} s & for \quad 0 < s \leq s_0 \\[2mm] \frac{\tau_0}{s_f - s_0}(s_f - s) & for \quad s_0 < s \leq s_f \\[2mm] 0 & for \quad s > s_f \end{cases} \tag{4}$$

where τ and s are the interfacial shear stress and its corresponding slip, respectively, τ_0 is the maximum interfacial shear stress, s_0 is the slip at τ_0 and s_f is the maximum slip of the τ-s relationship.

This study aimed to simulate the effects of sustained loading under SLS conditions. For this purpose, it was assumed that the slip between CFRP and concrete can be represented by a local bond-slip law applied to the adhesive layer, that the deformability of the concrete can be neglected and that the adhesive is subjected to pure shear [40, 45, 53, 56, 59–61]. The interfacial shear stress in the ascending branch of the bilinear bond-slip law can be obtained by:

$$\tau = K_e\, s \tag{5}$$

where s is the slip of the CFRP strip and K_e is the stiffness of the τ-s relationship,

291 that can be described as:

$$K_e = \tau_0/s_0 \tag{6}$$

292 being τ_0 and s_0 the maximum interfacial bond stress in the τ-s relationship and its
293 corresponding slip, respectively.

294   The first derivative of Eq. 5 yields:

$$\frac{d\tau}{dx} = K_e \, \varepsilon_f \tag{7}$$

295 where ε_f is the strains in FRP strip.

296

297   By using Eq. 7 and Eq. 1, the following differential equation can be obtained:

$$\frac{d^2\sigma_f}{dx^2} - \alpha^2\sigma_f = 0 \tag{8}$$

298 where

$$\alpha^2 = \frac{K_e}{E_f \, t_{eq}} \tag{9}$$

299 being E_f is the modulus of elasticity of the FRP.

300

301   Eq. 8 can be solved applying the following boundary conditions: at x=0 (free end),
302 $\sigma_f = 0$ and at x=L (loaded end), $\sigma = \sigma_0$ (the applied stress in the FRP). After solving
303 the distribution of the axial FRP stress, shear stress and the slip along the bonded
304 length (at any distance x from the free end) are given by:

$$\sigma_f(x) = \sigma_0 \, \frac{\sinh(\alpha x)}{\sinh(\alpha L_b)} \tag{10}$$

20

$$\tau(x) = t_{eq}\,\alpha\,\sigma_0\,\frac{\cosh(\alpha x)}{\sinh(\alpha L_b)} \tag{11}$$

$$s(x) = \frac{t_{eq}}{K_e}\,\alpha\,\sigma_0\,\frac{\cosh(\alpha x)}{\sinh(\alpha L_b)} \tag{12}$$

4.2. Bond behavior under sustained loading

The bases of the approach presented in [36] for modelling the long-term bond behavior of steel bars in concrete have been followed in this work, with the difference that the creep effects are introduced here into the bilinear bond-slip model for short-term behavior of the NSM system previously described (Fig. 11). According to this approach, the evolution of the local bond-slip with time can be estimated based on the initial local bond-slip law and the creep function of the joint, in such a way that slip at any time can be described by:

$$s(t) = s_0(1 + \phi(t, t_0)) \tag{13}$$

where s(t_0) and s(t) are the slip values at time t_0 and t from loading, respectively, and $\phi(t, t_0)$ is the creep function of the joint at time t with respect to time t_0.

The application of this assumption to the short-term bond-slip model (Fig. 11) would cause a shift on the right of the curve for t_0, resulting in a set of curves for different times as indicated in Fig. 12. Nevertheless, to avoid an unrealistic increment in the available energy under long-term loading (area under the curves), the use of the bond-slip law at time t_0 as an envelope was proposed, meaning that the maximum available energy corresponds to short-term bond law [36]. Therefore the final set of curves for long-term would correspond to the modified ascending branches for each time t intersecting with the descending branch for short-term as indicated in Fig. 12. This

21

³²³ assumption was shown to be adequate in previous works using a non-linear bond-slip

³²⁴ law composed of four zones, similar to that used for deformed steel bars in concrete
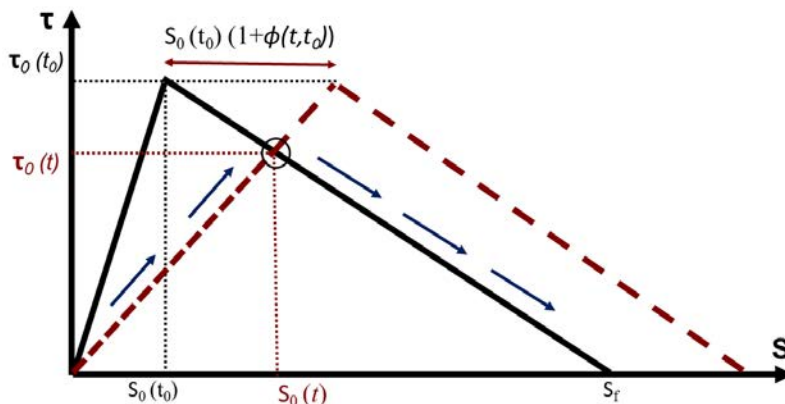
³²⁵ [35].

Fig. 12: Bond-slip evolution with time (Arrows show the new bond-slip law at time t)

³²⁶ The practical application of this methodology can be carried out using the so-

³²⁷ called Effective Modulus Method (EMM) in which an effective stiffness $K_e(t)$ [40] for

³²⁸ the ascending branch is used as follows:

$$K_e(t) = \frac{K_e(t_0)}{(1 + \phi(t, t_0))} \tag{14}$$

³²⁹

$$\tau_0(t) = K_e(t)\, s_0(t) \tag{15}$$

³³⁰ where $K_e(t_0)$ and $K_e(t)$ are the stiffness of the ascending branch at times t_0 and t,

³³¹ respectively, $\tau_0(t)$ and $\phi(t,t_0)$ are the maximum interfacial shear stress and the creep

³³² factor at time t, respectively, and $s_0(t)$ is the slip corresponding to $\tau_0(t)$.

³³³ This is represented in Fig. 12 through the reduction in the slope of the ascending

³³⁴ branch of the bond-slip relationship at time t $(t > t_0)$. With this reasoning, the

³³⁵ time-dependent behavior can be introduced in the analytical equations describing the

short-term bond problem (Eq. 9 to Eq. 12) just by changing the stiffness with time $(K_e(t))$.

The evolution of bond-slip law with time , presented in Fig. 12, is mainly dependent on the adhesive's properties. These properties can be determined through a tensile creep test that allows for creep coefficients at different times $(\phi(t))$ to be obtained, and therefore, for bond-slip relationships at any time to be determined. Through this procedure, the analytical equations describing the distribution of the axial CFRP stress, the shear stress and the slip along the bonded length with time read:

$$\alpha^2(t) = \frac{K_e(t)}{E_f \, t_{eq}} \tag{16}$$

$$\sigma_f(x,t) = \sigma_0 \, \frac{\sinh(\alpha(t) \, x)}{\sinh(\alpha(t) \, L_b)} \tag{17}$$

$$\tau(x,t) = t_{eq} \, \alpha(t) \, \sigma_0 \, \frac{\cosh(\alpha(t) \, x)}{\sinh(\alpha(t) \, L_b)} \tag{18}$$

$$s(x,t) = \frac{t_{eq}}{K_e(t)} \, \alpha(t) \, \sigma_0 \, \frac{\cosh(\alpha(t) \, x)}{\sinh(\alpha(t) \, L_b)} \tag{19}$$

Application of previous equations indicate that under sustained loading more creep in the joint develops with time, this leading to reduction in the effective stiffness and consequently more slip takes place along the bonded length and more bonded length is activated. Furthermore, this effect leads to a redistribution of stresses resulting in a decrease of the maximum shear and local concrete stresses.

5. Comparison between analytical and experimental results

The experimental results obtained in the current work are used to check the presented analytical model.

Assuming a short-term load-slip curve as that shown in Fig. 13 and that the axial stiffness of the FRP strip is much smaller than that of the concrete, the maximum bond-stress at time t_0 ($\tau_0(t_0)$) can be obtained as [40, 53]:

$$\tau_0(t_0) = \frac{P_{max}^2}{L_p \, A_f \, E_f \, s_f} \tag{20}$$

where P_{max} and s_f are the load and slip values at the peak point of the load-slip curve (i.e. point B) at which the interface shear stress reaches its maximum value, and s_0 is the slip at the end of the linear-elastic part of the curve (point A).
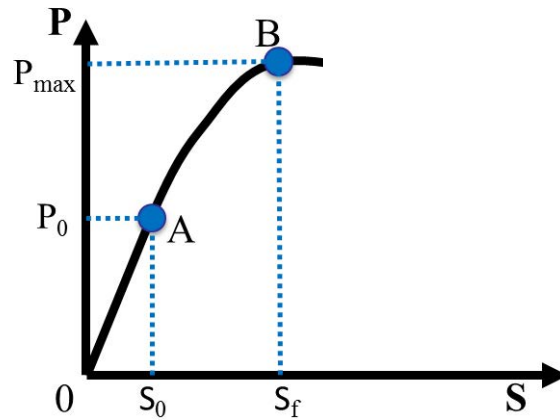

Fig. 13: Load-slip under monotonic loading

The adhesive's creep coefficients were obtained from a tensile creep test carried out by the authors [52] at the same environmental conditions as the pull-out tests and with the same batch of epoxy resin. Experimental values of creep coefficients and the corresponding equivalent stiffness are presented in the second and third columns of Table 2, respectively, while the bond-slip parameters ($\tau_f(t)$ and $s_0(t)$ in Fig. 12) for

24

the long-term equivalent curves at different times are indicated in the fourth and fifth columns, respectively.

Table 2: Bond-slip parameters at different times

Time (hours)	$\phi(t)$	$K_e(t)$ (N/mm^3)	$\tau_0(t)$ (MPa)	$s_0(t)$ (mm)
0	0	229	18.35	0.08
10	0.21	189	18.04	0.10
50	0.45	158	17.71	0.11
100	0.67	137	17.41	0.13
500	1.66	86	16.20	0.19
1000	2.40	68	15.42	0.23

Once the equivalent stiffness $(K_e(t))$ has been obtained, analytical predictions of the evolution of slip with time (Eq. 19) are compared to experimental values of the experimental program and presented in Fig. 14 to Fig. 16, for specimens with bonded length of 60, 90 and 120 mm, respectively. As it can be seen, good agreement is in general observed for the analyzed cases, thus indicating that the proposed methodology predicts reasonably well the slip evolution with time.

For the purpose of clarification, Table 3 presents a summary of experimental and predicted values for the loaded-end slips at loading (t=0 hours) and at the end of the testing period (t=1000 hours). The ratios between experimental and predicted slip values are also shown along with the mean and the standard deviation showing good correlation between experimental and analytical results.
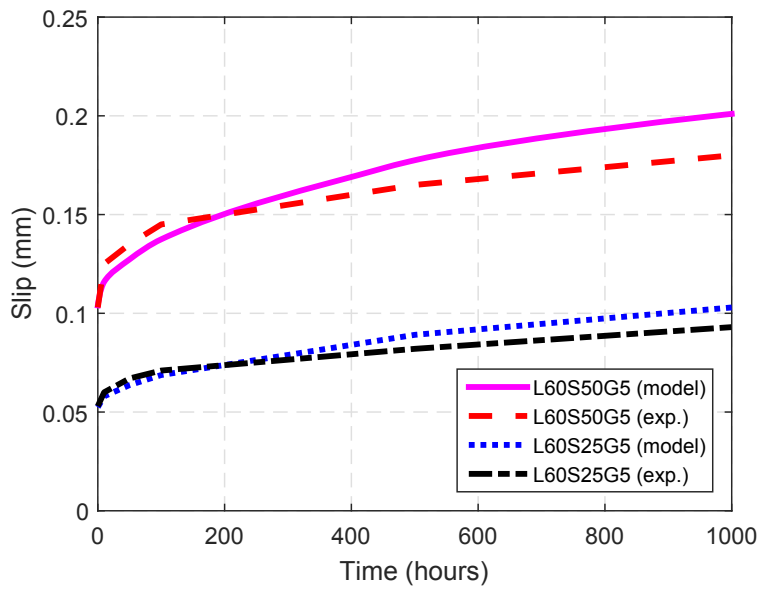
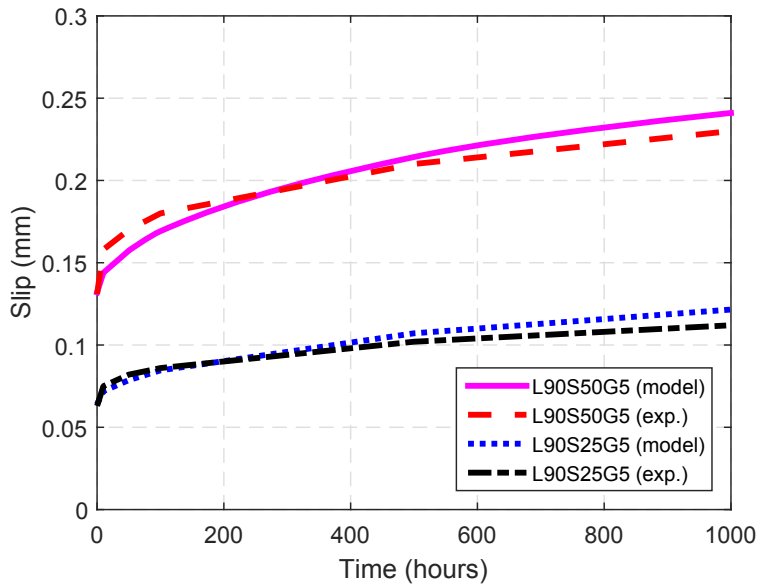Fig. 14: Comparison of analytical and experimental evolution of slip with time for specimens with L_b=60 mm

Fig. 15: Comparison of analytical and experimental evolution of slip with time for specimens with L_b=90 mm
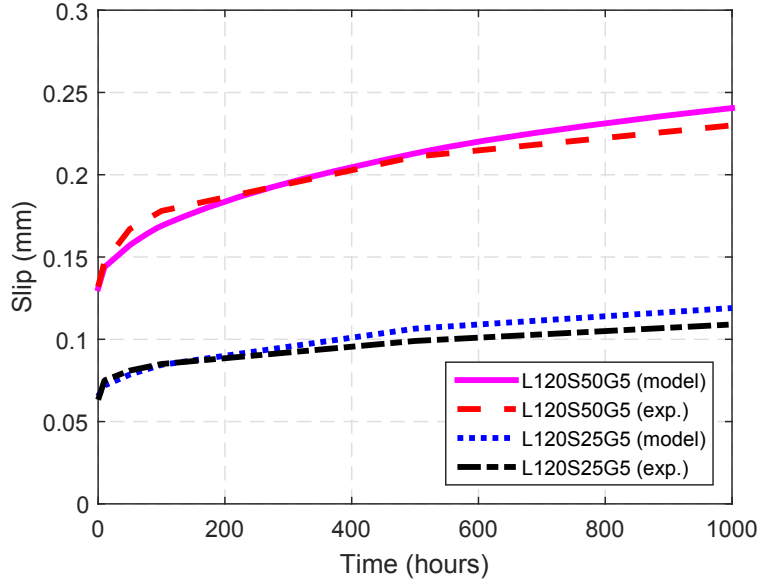
26

Fig. 16: Comparison of analytical and experimental evolution of slip with time for specimens with L_b=120 mm

Table 3: Comparison between experimental and analytical long-term predictions.

Specimen	loaded-end slip at t= 0 hours (mm)			loaded-end slip at t= 1000 hours (mm)		
	$s_{exp.}$	s_{model}	$s_{model}/s_{exp.}$	$s_{exp.}$	s_{model}	$s_{model}/s_{exp.}$
L60S25G5	0.053	0.052	0.98	0.094	0.103	1.10
L60S50G5	0.103	0.104	1.01	0.180	0.201	1.10
L90S25G5	0.063	0.064	1.02	0.112	0.122	1.09
L90S50G5	0.131	0.132	1.01	0.230	0.241	1.04
L120S25G5	0.063	0.064	1.02	0.109	0.119	1.09
L120S50G5	0.132	0.131	0.99	0.231	0.241	1.04
Mean			1.01			1.06
Standard deviation			0.01			0.04

27

6. Conclusions

Results of a study designed to investigate the time-dependent bond behavior between NSM FRP and concrete have been presented. Sustained load level (25% and 50% of the failure load), bonded length (60, 90 and 120 mm) and adhesive thickness were the main parameters studied. A simplified analytical methodology was introduced to predict the time-dependent behavior. From the specimens tested in the current study the following conclusions may be drawn:

- Specimens with bonded length equal to 90 and 120 mm showed similar behaviors within the same test condition.

- For all bonded lengths used, increasing the sustained loading level from 25% to 50% increased the total slip, by almost the double, at any time along the testing period. This observation is coherent with the monotonic test results obtained.

- When the groove width increased from 5 to 10 mm, the total slip values reduced for all bonded lengths. The average reduction was 0.82, 0.91 and 0.93 for specimen with L_b equal to 60, 90 and 120 mm, respectively.

- The ratio between the total slip at 1000 hours of sustained loading to the instantaneous slip at the time of application of the sustained load (t=0) was found to be similar for all specimens tested. The ratios obtained were 1.77, 1.77 and 1.88 for specimens subjected to sustained loading equal to 25% with L_b equal to 60, 90 and 120 mm, respectively, and 1.75, 1.76 and 1.75 in case of specimens subjected to sustained loading equal to 50% with L_b equal to 60, 90 and 120 mm, respectively.

- A simplified analytical methodology has been developed, based on a bi-linear interface model, using the effective modulus method. Good agreement is observed

28

between analytical and experimental results.

Acknowledgement

References

[1] Balaguru P, Nanni A, Giancaspro J. FRP composites for reinforced and prestressed concrete structures: A guide to fundamentals and design for repair and retrofit. CRC Press; 2008.

[2] Bank LC. Composites for construction: structural design with FRP materials. John Wiley & Sons; 2006.

[3] Teng J, Chen JF, Smith ST, Lam L. FRP: strengthened RC structures. Frontiers in Physics 2002;1.

[4] fib Bulletin 14 . Externally bonded FRP reinforcement for RC structures. design and use of externally bonded fibre reinforced polymer reinforcement (FRP EBR) for reinforced concrete structures. The International Federation for Structural Concrete (FIB). fib Task Group 9.3 FRP reinforcement for concrete structures. Lausanne, Switzerland; 2001.

[5] fib Bulletin 40 . FRP reinforcement in RC structures. The International Federation for Structural Concrete (FIB). fib Task Group 9.3, FRP reinforcement for concrete structures. Lausanne, Switzerland; 2007.

[6] Lorenzis LD, Nanni A. Characterization of FRP rods as near-surface mounted reinforcement. Journal of Composites for Construction 2001;5(2):114–21.

[7] Parretti R, Nanni A. Strengthening of RC members using near-surface mounted FRP composites: Design overview. Advances in Structural Engineering 2004;7(6):469–83.

[8] De Lorenzis L, Teng J. Near-surface mounted FRP reinforcement: An emerging technique for strengthening structures. Composites Part B: Engineering 2007;38(2):119–43.

[9] Barros JA, Dias SJ, Lima JL. Efficacy of CFRP-based techniques for the flexural and shear strengthening of concrete beams. Cement and Concrete Composites 2007;29(3):203–17.

[10] Bilotta A, Ceroni F, Di Ludovico M, Nigro E, Pecce M, Manfredi G. Bond efficiency of EBR and NSM FRP systems for strengthening concrete members. Journal of Composites for Construction 2011;15(5):757–72.

[11] Lee D, Cheng L, Yan-Gee Hui J. Bond characteristics of various NSM FRP reinforcements in concrete. Journal of Composites for Construction 2012;17(1):117–29.

[12] Kotynia R. Bond between FRP and concrete in reinforced concrete beams strengthened with near surface mounted and externally bonded reinforcement. Construction and Building Materials 2012;32:41–54.

[13] Zhang S, Teng JG, Yu T. Bond strength model for CFRP strips near-surface mounted to concrete. Journal of Composites for Construction 2013;18(3):401–3.

[14] Rezazadeh M, Cholostiakow S, Kotynia R, Barros J. Exploring new NSM reinforcements for the flexural strengthening of RC beams: Experimental and numerical research. Composite Structures 2016;141:132–45.

[15] Dalfré GM, Barros JA. NSM technique to increase the load carrying capacity of continuous RC slabs. Engineering Structures 2013;56:137–53.

[16] Szabó ZK, Balázs GL. Near surface mounted FRP reinforcement for strengthening of concrete structures. Periodica Polytechnica Civil Engineering 2007;51(1):33–8.

[17] Coelho MR, Sena-Cruz JM, Neves LA. A review on the bond behavior of FRP NSM systems in concrete. Construction and Building Materials 2015;93:1157–69.

[18] De Lorenzis L, Nanni A. Bond between near-surface mounted fiber-reinforced polymer rods and concrete in structural strengthenings. ACI Structural Journal 2002;99(2):123–32.

[19] Hassan T, Rizkalla S. Investigation of bond in concrete structures strengthened with near surface mounted carbon fiber reinforced polymer strips. Journal of composites for construction 2003;7(3):248–57.

[20] Galati D, De Lorenzis L. Effect of construction details on the bond performance of NSM FRP bars in concrete. Advances in Structural Engineering 2009;12(5):683–700.

[21] Teng J, De Lorenzis L, Wang B, Li R, Wong T, Lam L. Debonding failures of RC beams strengthened with near surface mounted CFRP strips. Journal of Composites for Construction 2006;10(2):92–105.

[22] De Lorenzis L, Lundgren K, Rizzo A. Anchorage length of near-surface mounted fiber-reinforced polymer bars for concrete strengthening - experimental investigation and numerical modeling. ACI Structural Journal 2004;101(2):269–78.

[23] Sena Cruz JM, Oliveira de Barros JA. Bond between near-surface mounted carbon-fiber-reinforced polymer laminate strips and concrete. Journal of Composites for Construction 2004;8(6):519–27.

[24] Sena Cruz JM, Barros JA, Gettu R, Azevedo AF. Bond behavior of near-surface mounted CFRP laminate strips under monotonic and cyclic loading. Journal of Composites for Construction 2006;10(4):295–303.

[25] Novidis D, Pantazopoulou S, Tentolouris E. Experimental study of bond of NSM-FRP reinforcement. Construction and Building Materials 2007;21(8):1760–70.

[26] Soliman SM, El-Salakawy E, Benmokrane B. Bond performance of near-surface-mounted FRP bars. Journal of Composites for Construction 2010;15(1):103–11.

[27] Sharaky I, Torres L, Baena M, Miàs C. An experimental study of different factors affecting the bond of NSM FRP bars in concrete. Composite Structures 2013;99:350–65.

[28] Torres L, Sharaky IA, Barris C, Baena M. Experimental study of the influence of adhesive properties and bond length on the bond behaviour of NSM FRP bars in concrete. Journal of Civil Engineering and Management 2016;22(6):808–17.

[29] Yan X, Miller B, Nanni A, Bakis C. Characterization of CFRP rods used as near surface mounted reinforcement. 8th International conference on structural faults and repair, Edinburgh (Scotland); 1999, p. CD–ROM version.

32

[30] De Lorenzis L, Rizzo A, La Tegola A. A modified pull-out test for bond of near-surface mounted FRP rods in concrete. Composites Part B: Engineering 2002;33(8):589–603.

[31] Szabó, Zsombor Kálmán and Balázs, György L . Importance of boundary conditions on bond of NSM reinforcement. In: rd fib Congress and PCI Annual Convention, May 29 to June 2, Washington DC, USA, full paper on CD-ROM (12 pages). 2010,.

[32] Costa I, Barros J. Critical analysis of fibre-reinforced polymer near-surface mounted double-shear pull-out tests. Strain 2013;49(4):299–312.

[33] Bilotta A, Ceroni F, Barros JA, Costa I, Palmieri A, Szabó ZK, et al. Bond of NSM FRP-strengthened concrete: Round robin test initiative. Journal of Composites for Construction 2015;20(1):04015261–16.

[34] Costa I, Barros JA. Assessment of the bond behaviour of nsm frp materials by pullout tests. In: First Middle East Conference on Smart Monitoring, Assessment and Rehabilitation of Civil Structures (SMAR 2011). International Society for Structural Health Monitoring of Intelligent Infrastructure (ISHMII); 2011, p. 1–9.

[35] Borchert K, Zilch K. Bond behaviour of NSM FRP strips in service. Structural Concrete 2008;9(3):127–42.

[36] CEB-1997 . Serviceability models - behaviour and modelling in serviceability limit states including repeated and sustainedloads. CEB, Bulletin d'information No. 235, Lausanne, Switzerland; 1997.

[37] Costa I, Barros J. Tensile creep of a structural epoxy adhesive: Experimental and analytical characterization. International Journal of Adhesion and Adhesives 2015;59:115–24.

[38] Silva P, Fernandes PMG, Sena-Cruz J, Azenha M, Barros JA. Creep behavior and durability of concrete elements strengthened with NSM CFRP strips. In: 7th International Conference on Fiber Reinforced Polymer (FRP) Composites in Civil Engineering (CICE 2014). 2014, p. 1–6.

[39] Derias M, El-Hacha R, Rizkalla S. Durability of NSM FRP strengthening systems for rc flexural members. In: 4th International Conference on Fiber Reinforced Polymer (FRP) Composites in Civil Engineering (CICE 2008), Zurich, Switzerland. 2008,.

[40] Mazzotti C, Savoia M. Stress redistribution along the interface between concrete and FRP subject to long-term loading. Advances in Structural Engineering 2009;12(5):651–61.

[41] Meshgin P, Choi KK, Taha MMR. Experimental and analytical investigations of creep of epoxy adhesive at the concrete–FRP interfaces. International Journal of Adhesion and Adhesives 2009;29(1):56–66.

[42] Dash S, Jeong Y, Lopez M, Bakis C. Experimental characterization of moisture, temperature and sustained loading on concrete-FRP bond performance. In: 11th International Symposium on Fiber Reinforced Polymer Reinforcement for Concrete Structures (FRPRCS-11), Guimarães, Portugal. 2013,.

[43] Jeong Y, Lee J, Kim W. Modeling and measurement of sustained loading and temperature-dependent deformation of carbon fiber-reinforced polymer bonded to concrete. Materials 2015;8(2):435–50.

[44] Seracino R, Raizal Saifulnaz M, Oehlers D. Generic debonding resistance of EB and NSM plate-to-concrete joints. Journal of Composites for Construction 2007;11(1):62–70.

34

[45] Sena Cruz JS, Barros J. Modeling of bond between near-surface mounted CFRP laminate strips and concrete. Computers & Structures 2004;82(17):1513–21.

[46] Seracino, Rudolf and Jones, Nicola M and Ali, MS and Page, Mark W and Oehlers, Deric J . Bond strength of near-surface mounted FRP strip-to-concrete joints. Journal of Composites for Construction 2007;11(4):401–9.

[47] Sena-Cruz, José and Silva, Patrícia and Fernandes, Pedro Miguel Gomes and Azenha, Miguel and Barros, Joaquim AO and Sousa, Christoph Fernandes and Castro, Fernando and Teixeira, Tiago André Nunes . Creep behavior of concrete elements strengthened with NSM CFRP laminate strips under different environmental conditions. In: FRPRCS-11: 11th International Symposium on Fiber Reinforced Polymer for Reinforced Concrete Structures. Universidade do Minho; 2013, p. 1–12.

[48] Fernandes, Pedro MG and Silva, Patrícia M and Sena-Cruz, José . Bond and flexural behavior of concrete elements strengthened with NSM CFRP laminate strips under fatigue loading. Engineering Structures 2015;84:350–61.

[49] UNE-EN-12390-3 . Testing hardened concrete - part 3: Compressive strength of test specimens. AENOR- Asociación Española de Normalización y Certificación; 2003.

[50] ISO-527-5 . Plastics - determination of tensile properties - part 5: Test conditions for unidirectional fibre-reinforced plastic composites. ISO International Organization for Standardization; 1997.

[51] ISO-527-2 . Plastics - determination of tensile properties - part 2: Test conditions. ISO International Organization for Standardization; 1993.

[52] Emara M, Torres L, Baena M, Barris C, Moawad M. Effect of sustained loading and environmental conditions on the creep behavior of an epoxy adhesive for concrete structures strengthened with CFRP laminates. Composites Part B: Engineering 2017;129:88–96.

[53] Yuan H, Teng J, Seracino R, Wu Z, Yao J. Full-range behavior of FRP-to-concrete bonded joints. Engineering structures 2004;26(5):553–65.

[54] Ali MM, Oehlers D, Griffith M, Seracino R. Interfacial stress transfer of near surface-mounted FRP-to-concrete joints. Engineering Structures 2008;30(7):1861–8.

[55] Monti G, Renzelli M, Luciani P. FRP adhesion in uncracked and cracked concrete zones. In: Fibre-Reinforced Polymer Reinforcement for Concrete Structures: (In 2 Volumes). World Scientific; 2003, p. 183–92.

[56] Lu X, Teng J, Ye L, Jiang J. Bond–slip models for FRP sheets/plates bonded to concrete. Engineering structures 2005;27(6):920–37.

[57] Bilotta A, Faella C, Martinelli E, Nigro E. Indirect identification method of bilinear interface laws for FRP bonded on a concrete substrate. Journal of Composites for Construction 2011;16(2):171–84.

[58] Ko H, Matthys S, Palmieri A, Sato Y. Development of a simplified bond stress–slip model for bonded FRP–concrete interfaces. Construction and Building Materials 2014;68:142–57.

[59] De Lorenzis L, Miller B, Nanni A. Bond of fiber-reinforced polymer laminates to concrete. ACI Materials Journal 2001;98:256–64.

581 [60] Capozucca R. On the strengthening of RC beams with near surface mounted
582   GFRP rods. Composite Structures 2014;117:143–55.

583 [61] Pan J, Wu YF. Analytical modeling of bond behavior between FRP plate and
584   concrete. Composites Part B: Engineering 2014;61:17–25.